

Results from a Search for Light-Mass Dark Matter with a p -Type Point Contact Germanium Detector

C. E. Aalseth,¹ P. S. Barbeau,² N. S. Bowden,³ B. Cabrera-Palmer,⁴ J. Colaresi,⁵ J. I. Collar,^{2,*} S. Dazeley,³ P. de Lurgio,⁶ J. E. Fast,¹ N. Fields,² C. H. Greenberg,² T. W. Hossbach,^{1,2} M. E. Keillor,¹ J. D. Kephart,¹ M. G. Marino,⁷ H. S. Miley,¹ M. L. Miller,⁷ J. L. Orrell,¹ D. C. Radford,⁸ D. Reyna,⁴ O. Tench,⁵ T. D. Van Wechel,⁷ J. F. Wilkerson,^{7,9} and K. M. Yocum⁵

(CoGeNT Collaboration)

¹*Pacific Northwest National Laboratory, Richland, Washington 99352, USA*

²*Kavli Institute for Cosmological Physics and Enrico Fermi Institute, University of Chicago, Chicago, Illinois 60637, USA*

³*Lawrence Livermore National Laboratory, Livermore, California 94550, USA*

⁴*Sandia National Laboratories, Livermore, California 94550, USA*

⁵*CANBERRA Industries, Meriden, Connecticut 06450, USA*

⁶*Argonne National Laboratory, Argonne, Illinois 60439, USA*

⁷*Center for Experimental Nuclear Physics and Astrophysics and Department of Physics, University of Washington, Seattle, Washington 98195, USA*

⁸*Oak Ridge National Laboratory, Oak Ridge, Tennessee 37831, USA*

⁹*Department of Physics and Astronomy, University of North Carolina, North Carolina 27599, USA*

(Received 14 March 2010; published 29 March 2011)

We report on several features in the energy spectrum from an ultralow-noise germanium detector operated deep underground. By implementing a new technique able to reject surface events, a number of cosmogenic peaks can be observed for the first time. We discuss an irreducible excess of bulklike events below 3 keV in ionization energy. These could be caused by unknown backgrounds, but also dark matter interactions consistent with DAMA/LIBRA. It is not yet possible to determine their origin. Improved constraints are placed on a cosmological origin for the DAMA/LIBRA effect.

DOI: 10.1103/PhysRevLett.106.131301

PACS numbers: 95.35.+d, 14.80.Va, 29.40.Wk, 95.55.Vj

We have recently presented first dark matter limits [1] from the operation of p -type point contact (PPC) germanium detectors. PPCs offer an unprecedented combination of large mass and modest electronic noise, resulting in an enhanced sensitivity to low-energy rare events. Promising applications in astroparticle and neutrino physics are expected [2]. Their role within light-mass particle dark matter searches is introduced in [1].

Detector radiocontamination became evident during operation of a PPC at a depth of 330 meters of water equivalent (mwe) [1]. A new 440 g PPC diode was built to address this. The new crystal is a modified BEGe (Broad Energy Germanium), a commercial quasiplanar PPC design from Canberra Industries. It is operated in the Soudan Underground Laboratory (2100 mwe). This detector, while still not featuring an electroformed cryostat, has delivered more than one order-of-magnitude background reduction compared to [1]. The background achieved below ~ 3 keVee (keV electron equivalent, i.e., ionization energy), down to the ~ 0.4 keVee electronic noise threshold, is so far the lowest reported by any dark matter detector. The shielding, electronics, and basic pulse-shape discrimination (PSD) are similar to [1], with the addition of storage of raw preamplifier traces, and removal of two internal active shields. Although an external muon veto is preserved,

veto-coincident events do not accumulate in excess near threshold. We do not apply veto cuts to these data, avoiding a dead time penalty.

A number of peaks are observed in low-energy spectra from ultralow-background germanium detectors. They originate in activation of the crystal by exposure to cosmogenic neutrons and protons at sea level. Long-lived radioactive products result from their spallation of germanium nuclei. Whenever this progeny decays via electron capture (EC), the deposited energy can be limited to the atomic binding energy of the daughter's captured electron, released as short-ranged x rays and Auger electrons. Taking place within the crystal, these are detected with $\sim 100\%$ efficiency, giving rise to the observed peaks.

Because of the short attenuation length (microns) expected from low-energy x rays and the exclusive use of radioclean materials near crystals, all low-energy peaks so far observed have an internal cosmogenic origin. For p -type diodes, an additional obstacle against external low-energy radiation is a quasi-inactive $n+$ contact, spanning most of the surface of the semiconductor. This contact is created by lithium diffusion down to a depth 0.5–1 mm. Figure 1 displays the decay of the 10.36 keV K -shell EC peak from ^{71}Ge , produced via intense thermal neutron activation of a PPC. A peak at 1.29 keV, originating in

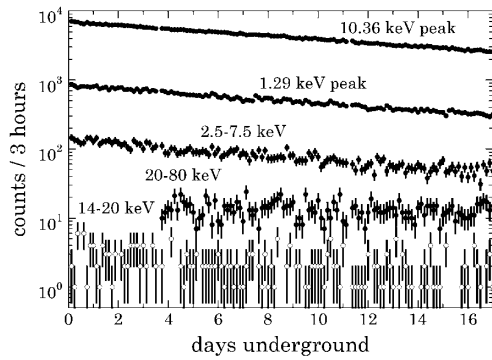


FIG. 1. Decays associated with ^{71}Ge ($T_{1/2} = 11.4$ d) produced via thermal neutron activation of the PPC in [1] (see text).

L -shell EC, exhibits the same decay (also the region 0.5–1.29 keV, not shown for clarity). So does the 2.5–7.5 keV “plateau”, but not events above 10.36 keV. The ratio of activity in the plateau to that under the 10.36 keV peak matches the estimated fraction of Li-diffused volume, suggesting an origin for most plateau events in partial charge collection from ^{71}Ge decays within the $n+$ contact.

Such partial energy depositions can create an issue, by accumulating in the region of interest for dark matter studies. In inspecting PPC preamplifier traces we noticed a population of low-energy slow pulses, with rise times (10% to 90% of maximum amplitude, t_{10-90}) significantly longer than the typical $t_{10-90} \sim 0.3 \mu\text{s}$. These are mentioned in early germanium detector literature as originating precisely in the $n+$ contact, being caused by weak electric fields next to the Li-diffused region [3]. We demonstrated the association between partial charge collection and slow rise time by irradiating the “closed end” [side opposite to $p+$ contact, Fig. 2 inset] of the PPC in [1] with ^{241}Am gammas. Figure 2 displays the longer rise times associated with partial energy depositions in the $n+$ contact from the short-ranged 59.5 keV gamma (attenuation ~ 1 mm). Full-energy depositions, happening deeper in the crystal, show the expected $t_{10-90} \sim 0.3 \mu\text{s}$. Using a simulation of the energy-depth profile in this calibration, the energy spectrum is faithfully reconstructed when the charge collection efficiency ϵ is described by a best-fit sigmoid $\epsilon = 1/[1 + 43.5e^{-86(d-0.14)}]$, where d is the interaction depth in cm. This implies an outermost “dead” layer of ~ 1 mm, followed by a ~ 1 mm “transition” layer prone to partial charge collection, as in [3]. Intending to reject surface events in this search via t_{10-90} cuts, we conservatively use a fiducial detector mass of 330 g (two outer mm discarded). We estimate the present uncertainty in this mass to be $\sim 10\%$.

Based on this discussion, low-energy (few keV) radiation can reach the PPC active volume through a single region, the intracontact passivated surface, at the center of which the 5 mm $p+$ point-contact is established [Fig. 2, inset]. The protective SiO_x passivation layer is just ~ 1500

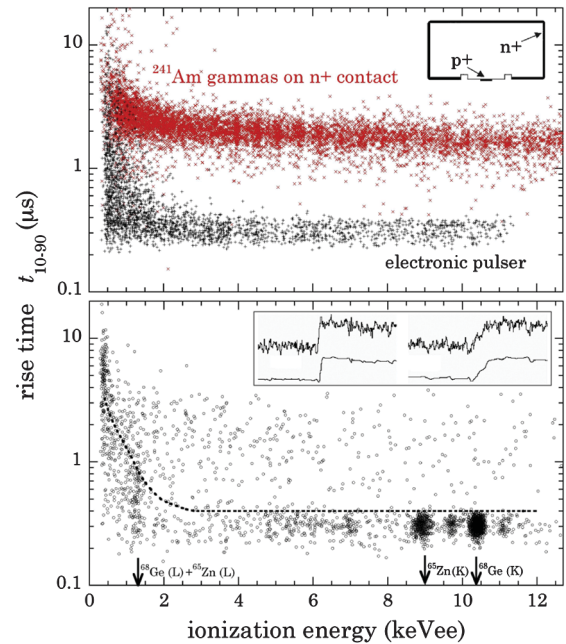


FIG. 2 (color). Top panel: Rise time in preamplifier traces from ^{241}Am gammas in the PPC in [1] and a manual scan of reference electronic pulser signals in the Soudan PPC (see text). Bottom panel: Background events collected by the PPC in Soudan. The dotted line represents the 90% signal acceptance contour for bulk events. Top inset: Vertical cross section of a cylindrical BEGe PPC, showing the two contacts. Bottom inset: Typical preamplifier traces from 1 keVee events, before and after wavelet denoising [19], for $t_{10-90} = 0.22 \mu\text{s}$ (left) and $t_{10-90} = 1.53 \mu\text{s}$ (right).

Angstroms thick. Any events arising from an external low-energy source must originate from materials in the line-of-sight of this surface (diameter 2.2 cm). These are specially-etched virgin PTFE, similarly treated OFHC copper and a needle contact (gold-plated brass, its tip wetted with low-background pure tin).

Figure 2 (bottom) shows the rise time distribution for low-energy events in the PPC at Soudan. These data correspond to an eight-week period starting three months after underground installation, to allow for ^{71}Ge decay. The top panel shows the same distribution for a collection of electronic pulser events in this detector. After a small upwards shift in t_{10-90} by $0.1 \mu\text{s}$, these strongly resemble radiation-induced bulk events ($t_{10-90} \sim 0.3 \mu\text{s}$) in this representation. The shift accounts for the additional charge collection time affecting energy depositions in the bulk of the crystal. Simulations of charge collection corroborated the magnitude of the applied shift. The dotted line in the bottom panel represents the 90% boundary for pulser signal acceptance. Further confirmation that this acceptance applies to bulk events is obtained from the preservation of the L -shell EC activity from ^{68}Ge (1.29 keV) and ^{65}Zn (1.1 keV) following this rise time cut. While this confirms that bulk event acceptance is understood down to 1 keV, the possibility remains of some unrejected surface

events closer to threshold. A comparison with the distribution of ^{241}Am surface events [Fig. 2] indicates that any such contamination should be modest.

Figure 3 displays Soudan spectra after the 90% signal acceptance rise time cut in Fig. 2, which generates a factor 2–3 reduction in background. This residual spectrum is dominated by events in the bulk of the crystal, like those from neutron scattering, cosmogenic activation, dark matter interactions, or unknown backgrounds. Several cosmogenic peaks are revealed for the first time. All expected cosmogenic products capable of a monochromatic signature are indicated. Observable activities are incipient for all.

We employ the methods in [1] to obtain weakly interacting massive particle (WIMP) and axion-like particle dark matter limits from this spectrum. The energy region used to extract WIMP limits is 0.4–3.2 keVee (from threshold to full range of the highest-gain digitization channel). A correction is applied to compensate for signal acceptance loss from cumulative data cuts [solid sigmoid in Fig. 3, inset]. The model adopted to fit the data consists of a response function for each WIMP mass [1] with a free spin-independent cross section, free exponential and constant terms, and two Gaussians to account for ^{65}Zn and ^{68}Ge L -shell EC. The energy resolution is defined by $\sigma_n = 69.4$ eV and $F = 0.29$ (same notation as [1]). The assumption of an irreducible exponential background is

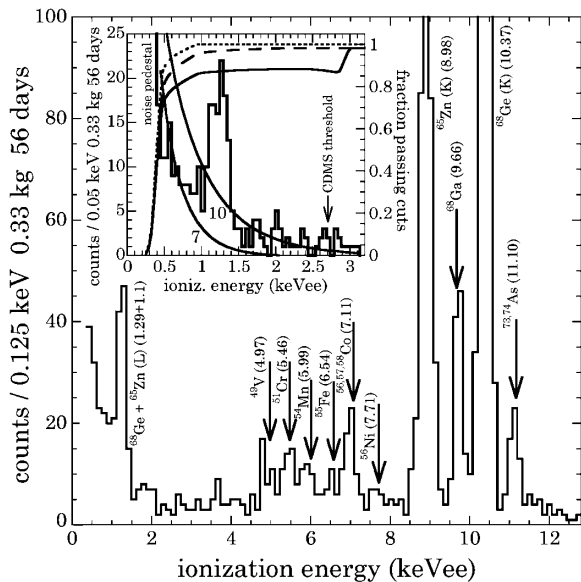


FIG. 3. Low-energy spectrum after all cuts, prior to efficiency corrections. Arrows indicate expected energies for all viable cosmogenic peaks (see text). Inset: Expanded threshold region, showing the ^{65}Zn and ^{68}Ge L -shell EC peaks. Overlapped on the spectrum are the sigmoids for triggering efficiency (dotted), trigger + microphonic PSD cuts [1] (dashed) and trigger + PSD + rise time cuts (solid), obtained via high-statistics electronic pulser calibrations. Also shown are uncorrected reference signals from 7 GeV/c^2 and 10 GeV/c^2 WIMPs with spin-independent coupling $\sigma_{\text{SI}} = 10^{-4}$ pb.

justified, given the mentioned possibility of some residual surface events and the accumulation towards threshold they exhibit. A second source of background possibly unaccounted for are L -shell EC activities from cosmogenics lighter than ^{65}Zn . These are expected to contribute $<10\%$ of the 0.5–0.9 keVee rate (their L -shell to K -shell EC ratio is $\sim 11\%$ [4]). Another possibility, discussed below, are recoils from unvetted muon-induced neutrons.

Figure 4 (top) displays the extracted sensitivity in spin-independent coupling (σ_{SI}) vs WIMP mass (m_χ). For m_χ in the range ~ 7 –11 GeV/c^2 the best-fit to the WIMP coupling acquires a value with a lower 90% C.L. interval incompatible with zero. The upper and lower 90% C.L. intervals for the coupling define the red contour in Fig. 4. For example, the best fit for $m_\chi = 9 \text{ GeV}/c^2$ provides a reduced chi-square $\chi^2/dof = 20.1/18$ at $\sigma_{\text{SI}} = 6.7(\pm 1.2) \times 10^{-41} \text{ cm}^2$. However, the null hypothesis (same background model minus the WIMP response)

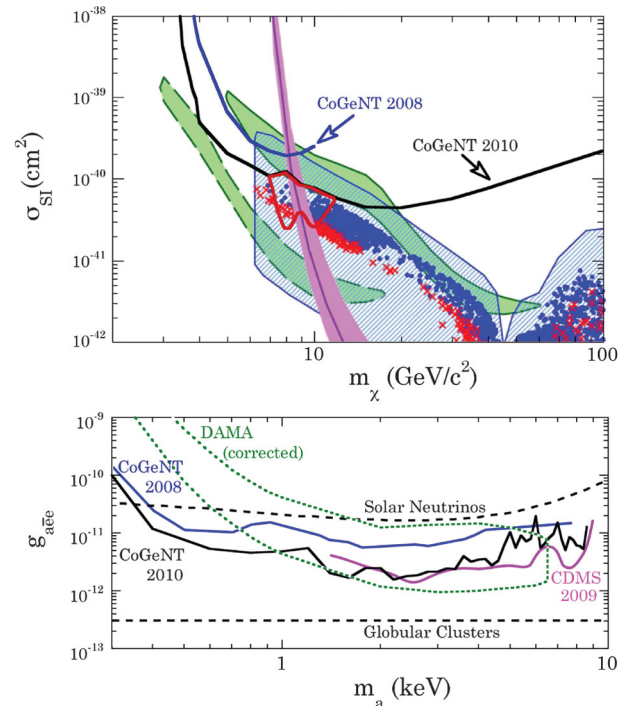


FIG. 4 (color). Top panel: 90% C.L. WIMP exclusion limits from CoGeNT overlaid on Fig. 1 from [5]. Green shaded patches denote the phase space favoring the DAMA/LIBRA annual modulation (the dashed contour includes ion channeling). Their exact position has been subject to revisions [20]. The violet band is the region supporting the two CDMS candidate events. The scatter plot and the blue hatched region represent the supersymmetric models in [6] and their uncertainties, respectively. Models including WIMPs with $m_\chi \sim 7$ –11 GeV/c^2 provide a good fit to CoGeNT data (red contour, see text). The relevance of XENON10 constraints in this low-mass region has been questioned [21]. Bottom panel: Limits on axioelectric coupling $g_{a\bar{e}e}$ for pseudoscalars of mass m_a composing a dark isothermal galactic halo (see text).

yields a similar $\chi^2/dof = 20.4/20$, the result of the WIMP response being nearly exponential in shape. Based on the quality of fits, it is not possible to distinguish between an unknown background and dark matter.

It has been recently emphasized [5] that light WIMP models [1,6,7] provide a common explanation to the DAMA/LIBRA annual modulation effect [8] and the modest excess of signal-like events in CDMS [9]. Such WIMP candidates are compatible with CoGeNT data [Fig. 4]. When interpreted as WIMP interactions, the low energy (3.3 and 4.2 keVee) of the CDMS recoil-like events is suggestive of a light WIMP. However, the 2.7 keVee CDMS threshold [Fig. 3, inset] does not allow for a ready identification of such candidates.

Figure 4 (bottom) shows limits on axioelectric dark matter couplings, extracted as in [1] from the region 0.5–8.5 keVee. Sensitivity to this coupling should improve with additional exposure. A discussion on the relevance of the DAMA/LIBRA-favored region in this phase space is provided in [10]. Lastly, we refer to [1] for a criticism of ion channeling [Fig. 4] as part of the DAMA/LIBRA effect. In light of our improved sensitivity, a fair treatment of this possibility (i.e., including channeling also for germanium crystals) should render it highly constrained.

Enticing as it is to contemplate cosmological implications from unexpected low-energy spectral features, our focus must remain on finding less exotic explanations. One evident possibility is a contribution from recoils caused by environmental or muon-induced neutrons. Simulated transport of the environmental neutron flux at Soudan [11] through our shielding generates a prediction short of the observed low-energy rise by ~ 100 . This prediction matches other studies at the same overburden [12]. The muon-induced contribution prior to vetoing is simulated following [12,13], yielding just 7% of the rate at threshold (the observed muon veto coincidences limit this to $< 15\%$). Partial energy depositions from high energy gammas are not expected to accumulate in this spectral region [14]. Other possibilities, including alpha recoils from radon deposition on the passivated surface, degraded beta emissions from ^{40}K in PTFE, excess ^{210}Po [15] on the specially selected tin at the central contact, etc., have been studied and found lacking. The hypothesis that the rise might be due to unrejected electronic noise would involve a dramatic deviation from expectations [16]. Pulses comprising the rise are asymptomatic [Fig. 2, inset]. One conjecture worth investigation is the effect of a possible surface channel on the intracontact surface [17], perhaps leading to degraded energy events that might escape rise time cuts.

In conclusion, we have presented improved experimental constraints on light-mass dark matter candidates. After rejection of dominant surface backgrounds, an unexplained excess persists in the low-energy spectrum. In view of its apparent agreement with existing WIMP models, a claim and a glimmer of dark matter detection in two other

experiments, it is tempting to consider a cosmological origin. Past experience prompts us to exhaust less exotic possibilities. If this feature originates in dark matter interactions, a PPC-based MAJORANA DEMONSTRATOR [18] would detect an annual modulation effect in both rate and average energy deposited.

Work sponsored by NSF Grants No. PHY-0653605, No. PHY-0239812, No. PHY-0114422, LLNL Contract No. DE-AC52-07NA27344, LDRD programs at SNL and PNNL, and the Office of Nuclear Physics, U.S. DOE. N. F. is supported by the DOE/NNSA SSGF program SAND Number: 2010-1375J, LLNL-JRNL-425007. We owe gratitude to all personnel at the Soudan Underground Laboratory.

*collar@uchicago.edu

- [1] C. E. Aalseth *et al.*, *Phys. Rev. Lett.* **101**, 251301 (2008); **102**, 109903(E) (2009).
- [2] P. S. Barbeau *et al.*, *J. Cosmol. Astropart. Phys.* **09** (2007) 009.
- [3] E. Sakai, *IEEE Trans. Nucl. Sci.* **18**, 208 (1971) and Refs. therein.
- [4] J. N. Bahcall, *Phys. Rev.* **132**, 362 (1963).
- [5] A. Bottino *et al.*, *Phys. Rev. D* **81**, 107302 (2010).
- [6] A. Bottino *et al.*, *Phys. Rev. D* **78**, 083520 (2008).
- [7] G. Gelmini, A. Kusenko, and S. Nussinov, *Phys. Rev. Lett.* **89**, 101302 (2002); R. Foot, *Phys. Rev. D* **69**, 036001 (2004); C. Bird *et al.*, *Mod. Phys. Lett. A* **21**, 457 (2006); J. F. Gunion, D. Hooper, and B. McElrath, *Phys. Rev. D* **73**, 015011 (2006); J. L. Feng and J. Kumar, *Phys. Rev. Lett.* **101**, 231301 (2008); S. Andreas *et al.*, *J. Cosmol. Astropart. Phys.* **10** (2008) 034; D. G. Cerdeño and O. Seto, *J. Cosmol. Astropart. Phys.* **08** (2009) 032; D. E. Kaplan, M. A. Luty, and K. M. Zurek, *Phys. Rev. D* **79**, 115016 (2009); Y. G. Kim *et al.*, *J. High Energy Phys.* **05** (2009) 036.
- [8] R. Bernabei *et al.*, *Eur. Phys. J. C* **56**, 333 (2008).
- [9] Z. Ahmed *et al.*, *Science* **327**, 1619 (2010).
- [10] J. I. Collar and M. G. Marino, arXiv:0903.5068.
- [11] S. Eichblatt, report CDMS 97-01-25, January 1997; H. Wulandari *et al.*, *Astropart. Phys.* **22**, 313 (2004).
- [12] J. M. Carmona *et al.*, *Astropart. Phys.* **21**, 523 (2004).
- [13] D. M. Mei and A. Hime, *Phys. Rev. D* **73**, 053004 (2006).
- [14] J. I. Collar, Ph.D. dissertation, University of South Carolina, 1992; H. V. Klapdor-Kleingrothaus *et al.*, *Nucl. Instrum. Methods Phys. Res., Sect. A* **481**, 149 (2002).
- [15] R. L. Brodzinski *et al.*, *Nucl. Instrum. Methods Phys. Res., Sect. A* **254**, 472 (1987).
- [16] P. J. Statham, *X-Ray Spectrom.* **6**, 94 (1977).
- [17] H. L. Malm and R. J. Dinger, *IEEE Trans. Nucl. Sci.* **23**, 75 (1976).
- [18] S. R. Elliott *et al.*, arXiv:0807.1741.
- [19] LabVIEW Advanced Signal Processing Toolkit.
- [20] J. L. Feng *et al.*, *J. Cosmol. Astropart. Phys.* **01** (2009) 032; D. Hooper *et al.*, *Phys. Rev. D* **79**, 015010 (2009).
- [21] A. Manzur *et al.*, *Phys. Rev. C* **81**, 025808 (2010).